Clim. Past Discuss., 9, 4705–4744, 2013
www.clim-past-discuss.net/9/4705/2013/
doi:10.5194/cpd-9-4705-2013

Climate of the Past
Discussions
Open Access

Investigating vegetation-climate feedbacks during the early Eocene

C. A. Loptson[1], **D. J. Lunt**[1], **and J. E. Francis**[2]

[1]School of Geographical Sciences, University Road, Bristol, BS8 1SS, UK
[2]School of Earth and Environment, University of Leeds, Leeds, LS2 9JT, UK

Received: 26 July 2013 – Accepted: 2 August 2013 – Published: 14 August 2013

Correspondence to: C. A. Loptson (c.loptson@bristol.ac.uk)

Published by Copernicus Publications on behalf of the European Geosciences Union.

Abstract

Evidence suggests that the early Eocene was a time of extreme global warmth, extending to the high latitudes. However, there are discrepancies between the results of many previous modelling studies and the proxy data at high latitudes, with models struggling to simulate the shallow temperature gradients of this time period to the same extent as the proxies indicate. Vegetation-climate feedbacks play an important role in the present day, but are often neglected in paleoclimate modelling studies and this may be a contributing factor to resolving the model-data discrepancy.

Here we investigate these vegetation-climate feedbacks by carrying out simulations of the early Eocene climate at 2 × and 4 × pre-industrial atmospheric CO_2 with fixed vegetation (homogeneous shrubs everywhere) and dynamic vegetation.

The results show that the simulations with dynamic vegetation are warmer in the global annual mean than the simulations with fixed shrubs by 0.9 °C at 2 × and 1.8 °C at 4 ×. In addition, the warming when CO_2 is doubled from 2 × to 4 × is 1 °C higher (in the global annual mean) with dynamic vegetation than with fixed shrubs. This corresponds to an increase in climate sensitivity of 26 %. This difference in warming is enhanced at high latitudes, with temperatures increasing by over 50 % in some regions of Antarctica. In the Arctic, ice-albedo feedbacks are responsible for the majority of this warming. On a global scale, energy balance analysis shows that the enhanced warming with dynamic vegetation is mainly associated with an increase in atmospheric water vapour but changes in clouds also contribute to the temperature increase. It is likely that changes in surface albedo due to changes in vegetation cover resulted in an initial warming which triggered these water vapour feedbacks.

In conclusion, dynamic vegetation goes some way to resolving the discrepancy, but our modelled temperatures cannot reach the same warmth as the data suggests in the Arctic. This suggests that there are additional mechanisms, not included in this modelling framework, behind the polar warmth.

CPD
9, 4705–4744, 2013

1 Introduction

The warmest climates of the past 65 million years occurred during the early Eocene (56–48 Ma) (Sloan and Morrill, 1998; Huber and Caballero, 2011), with benthic foraminifera indicating deep water temperatures of around 10 °C (Zachos et al., 2001) compared to between 2 and 3 °C in the present day (Martin et al., 2002). It is probable that there was little or no permanent ice, even at polar regions (Zachos et al., 2001, 2006). Atmospheric carbon dioxide levels were higher during the early Eocene compared to today, with proxy derived estimates ranging from 300 to over 4000 ppm (Beerling and Royer, 2011; Lowenstein and Demicco, 2006; Pagani et al., 2009; Sluijs et al., 2006; Pearson et al., 2007).

The latitudinal temperature gradients were much shallower than the present day (Bijl et al., 2009). Equatorial regions were only slightly warmer, with sea surface temperatures (SSTs) of 30–35 °C compared to the present day values of 25–30 °C (Pearson et al., 2007), but high latitudes were much warmer with SST estimates of 17 or 18 °C in the Arctic during the early Eocene (Sluijs et al., 2008). Until recently, models have had great difficulty in replicating this feature of the climate, instead producing temperatures that are cooler than indicated by the data in the high latitudes or temperatures that are higher than indicated by the proxies in the tropics (e.g. Heinemann et al., 2009; Winguth et al., 2010; Shellito et al., 2009; Roberts et al., 2009). This is due to the fact that the specific mechanisms that cause this shallow temperature gradient are unknown or not fully understood so cannot be accounted for (Winguth et al., 2010; Beerling et al., 2011; Sloan and Morrill, 1998).

To date, there have been several attempts to model the early Eocene climate. So far no models have been completely consistent with the evidence and data available. Some models are capable of reproducing some characteristics of the early Eocene climate, but do not fully explain the mechanisms behind it. Good agreement between proxy data and model results was achieved by Huber and Caballero (2011) except at some high latitude and all deep-sea locations. However, the CO_2 level prescribed in

CPD
9, 4705–4744, 2013

the model (4480 ppm) is at the upper limit of proxy predictions (Huber, 2008; Jaramillo et al., 2010; Pearson et al., 2007).

There have been several suggested mechanisms for the relatively warm high latitudes, including enhanced poleward heat transport, polar stratospheric clouds (Sloan and Pollard, 1998), aerosols (Kump and Pollard, 2008) and vegetation feedbacks (Otto-Bliesner and Upchurch, 1997).

There is increasing evidence that cloud feedbacks were a crucial mechanism for the high latitude warmth during the early Eocene. Sagoo et al. (2013) carried out a perturbed physics ensemble for the early Eocene using FAMOUS (Gordon et al., 2000; Pope et al., 2000). In the warmest early Eocene simulations, which also had the smallest root mean square (RMS) error when compared with proxy data, SSTs were over predicted in the tropics and under predicted at high latitudes (in the Arctic, Waipara river off New Zealand and in the South West Pacific). They found the warmer simulations had more cloud cover at high latitudes and concluded that although many aspects contribute to the overall warmth, the climate was very sensitive to cloud cover and associated albedo feedbacks.

Kiehl and Shields (2013) looked at the effect of changing cloud condensation nuclei on climate. Aerosol properties could have been significantly different in the early Eocene compared with today due to different vegetation distributions, desert regions, surface wind patterns and ocean productivity (Kiehl and Shields, 2013). However, it is not known exactly how these aerosol properties were different from today. By carrying out sensitivity studies using CCSM3 (Collins et al., 2006), Kiehl and Shields (2013) found that decreasing the cloud drop density and increasing the effective liquid cloud drop radius resulted in a temperature increase of 7 to 9 °C at high latitudes. This CCN effect produced the second largest warming effect, with increasing CO_2 producing the largest warming.

However, previous modelling studies for the early Eocene, such as those included in the EoMIP study (Lunt et al., 2012), have generally neglected vegetation feedbacks. These experiments used a fixed vegetation distribution of either one vegetation type

CPD
9, 4705–4744, 2013

covering all land (e.g. homogeneous shrubland as in the HadCM simulations) or a "best guess" distribution such as that of Sewall et al. (2000). Vegetation can have a significant effect on the climate (Bonan, 2008). Boreal forests have a larger biogeophysical effect than other biomes on annual mean global temperature due to albedo effects when snow is present; the trees, which have a low albedo, mask the high albedo of snow during the winter. Evapotranspiration has a cooling effect through cloud and precipitation feedbacks. The overall impact on climate (i.e. whether the net feedback is positive or negative) depends on the type of forest present. For example, tropical forests are a negative climate forcing because the cooling effect of evapotranspiration is greater than the warming due to the low forest albedo whereas boreal forests amplify warming because the albedo contribution dominates (Bonan, 2008). Simulations with dynamic vegetation have been carried out for other past time periods. For example, Zhou et al. (2012) investigated the effects of incorporating dynamic vegetation into Cretaceous simulations and found that the simulations with dynamic vegetation were 0.9 °C warmer with levels of precipitation 0.11 mm day^{-1} higher (relative to bare ground). Therefore, it is important that an accurate representation of vegetation is included in a GCM (general circulation model).

There are also potential problems with the data, as proxies are not fully understood and the interpretations may be subject to bias. For example, foraminifera may have undergone diagenetic alteration after deposition, which affects their isotopic composition, and therefore has an impact on inferred temperatures (Pearson et al., 2007). It is thought that some proxies may have a bias towards summer temperatures, e.g. the MBT-CBT proxy (Eberle et al., 2010). In addition, many of the species of foraminifera used to infer paleoclimate are extinct, so it is impossible to know whether the values recorded by them are equilibrium values (Roberts et al., 2009). One of the most recently developed paleothermometers uses organic compounds (archaeal-derived isoprenoid glycerol dibiphytanyl glycerol tetraethers or GDGTs) to measure SSTs. There are multiple calibrations for this proxy, and determining the most appropriate calibration can be difficult. Currently there are three different calibrations based on different ratios

Discussion Paper | Discussion Paper | Discussion Paper | Discussion Paper |

CPD
9, 4705–4744, 2013

Investigating vegetation-climate feedbacks during the early Eocene

C. A. Loptson et al.

of GDGTs: TEX_{86}^{L}, TEX_{86}^{H} (Kim et al., 2010) and “1/TEX_{86}”, a non-linear calibration (Liu et al., 2009), revised by Kim et al. (2010). This proxy is not fully understood, and as a result it is uncertain which calibration is most suitable for the early Eocene (Lunt et al., 2012; Hollis et al., 2012).

There can be a large difference in vegetation between early and mid-Eocene at high latitudes. Contreras et al. (2013) describe how the vegetation type changes from paratropical to cool temperate type vegetation between the early and middle Eocene. This rapid change in vegetation means that the dating of Eocene fossil flora and pollen needs to be robust when carrying out comparisons between models and data.

Due to all of the feedbacks between vegetation and the climate, it is very important to include a dynamic vegetation component to climate model simulations and that this representation of the vegetation within the model is sensible and realistic, i.e. the distribution and type of vegetation present in the model shows good agreement with available fossil evidence.

This study addresses four main questions: (1) is the modelled vegetation distribution consistent with available data? (2) What is the effect on early Eocene climate when interactive vegetation is included in the coupled ocean-atmosphere GCM HadCM3L? (3) Does incorporating dynamic vegetation reduce the temperature discrepancy between models and data for this time period? (4) What are the reasons behind the changes in temperature when CO_2 is doubled and when dynamic vegetation is coupled to HadCM3L? First, the predicted vegetation distributions are presented. We then investigate the effects of dynamic vegetation on climate by comparing simulations with fixed, prescribed vegetation to simulations that are fully coupled to a dynamic vegetation model. The results of all simulations are then compared to terrestrial and marine proxy data in order to assess the effectiveness of dynamic vegetation in reducing the model-data discrepancy. Energy balance analysis is carried out to diagnose the mechanisms that contribute to the temperature differences between simulations.

CPD
9, 4705–4744, 2013

2 Methods

The GCM used in this study is the UK Met Office General Circulation Model, HadCM3L (version 4.5), which has already been used in several paleoclimate studies of the early Eocene (Tindall et al., 2010; Lunt et al., 2012, 2010a,b). In this study the land surface scheme MOSES 2.1 was used, whereas MOSES 2.2 was used previously (see Essery et al. (2001) for a description of MOSES 2). The land surface scheme was changed because MOSES 2.1 is required for coupling the GCM to the dynamic vegetation model.

HadCM3L is a coupled atmosphere-ocean model with a resolution of 3.75° in longitude and 2.5° in latitude in both the atmosphere and ocean. The GCM has 19 vertical levels in the atmosphere and 20 in the ocean.

The paleogeography used was created using similar methods to that of Markwick and Valdes (2004). The Arctic is closed in this paleogeography (i.e. no flow is allowed into or out of the Arctic sea). The regions of maximum orographic height are on the West coast of North America (~3300 m) and in the centre of Antarctica (~2000 m).

The dynamic global vegetation model used was TRIFFID (Top-down Representation of Interactive Foliage and Flora Including Dynamics) (Cox, 2001). TRIFFID models the soil carbon, structure and percentage of the model gridbox occupied by each plant functional type (PFT). The five PFTs simulated by TRIFFID are broadleaf tree, needleleaf tree, C_3 grass, C_4 grass and shrub. The amount of soil carbon available to the vegetation is increased through litterfall (comprised of leaf, root and stem carbon) and microbial respiration returns soil carbon to the atmosphere at a rate determined by soil moisture and temperature. TRIFFID updates the vegetation and soil carbon every 10 days based on these carbon fluxes (calculated by the land surface model, MOSES 2.1) and competition between functional types. This information is then fed back to MOSES 2.1. This method verifies that the surface hydrological states experienced by the atmosphere and vegetation are consistent (Cox, 2001).

There is no strong evidence for the existence (or widespread growth) of C_4 grasses during the early Eocene (Christin et al., 2011; Edwards et al., 2010; Vicentini

CPD
9, 4705–4744, 2013

et al., 2008). Instead of C_4 grasses, it is likely that ferns would have grown instead (Donnadieu et al., 2009). In these experiments, C_3 and C_4 grasses have been combined into a single PFT ("grasses") to represent general low-level ground cover.

In order to investigate the effects of increased atmospheric CO_2 concentrations on the climate alone, two Eocene simulations were carried out with prescribed, fixed vegetation (homogeneous shrubs) covering all areas of land. One simulation was run with 2 × pre-industrial (PI) atmospheric CO_2 (560 ppm) and the other with 4 × PI CO_2 levels (1120 ppm). These will be referred to as 2 × SHRUB and 4 × SHRUB respectively. These CO_2 concentrations were chosen because they span part of the estimated range of atmospheric CO_2 during the early Eocene.

These simulations with fixed vegetation are a continuation of a set of simulations already in a quasi-steady-state, integrated for more than 3400 yr (Lunt et al., 2010a). Continuations of the 2 × SHRUB and 4×SHRUB were then run, but with HadCM3L coupled to TRIFFID, until the climate system equilibrated (1000 yr). This was done for both CO_2 levels, and these simulations will be referred to as 2 × DYN and 4 × DYN.

Changes in climate between 2 × DYN and 4 × DYN will inevitably be due to a combination of factors, including increased CO_2 and differing vegetation distributions. In order to separate these effects, a further simulation was carried out where the vegetation was prescribed to be the same as the 2 × DYN simulation, but the model was run with 4 × PI CO_2 . It was run for 550 model years. This simulation will be called FIXED. All experimental setups are summarised in table 1.

3 Results

3.1 Predicted vegetation

Figures 1 and 2 show the global vegetation distributions predicted by TRIFFID for 2 × DYN and 4 × DYN respectively. It can be seen that broadleaf and needleleaf trees move poleward when atmospheric CO_2 is doubled from 2 × to 4 × PI CO_2 . In contrast,

CPD
9, 4705–4744, 2013

Investigating vegetation-climate feedbacks during the early Eocene

C. A. Loptson et al.

shrubs move towards the equator. The extent of bare soil increases at low latitudes and grasses disappear almost entirely from Antarctica.

In both the Arctic and Antarctic, 4 × DYN shows broadleaf trees being the dominant PFT where shrubs and grasses had dominated in 2 × DYN. Grasses generally dominate in the tropics in both simulations but in 4 × DYN the area dominated by grasses increases to cover more of the equatorial regions. This is most noticeable in South East Asia and South America.

Evidence of plants from the early Eocene has been discovered from various locations worldwide and allows a comparison to be carried out between the modelled vegetation distribution and identified plant fossils from the literature.

Fossil evidence suggests that vegetation on the Antarctic Peninsula was mixed broadleaf and coniferous deciduous forest (Francis and Poole, 2002) and on the Antarctic Wilkes Land margin, there is evidence of paratropical forest in the early Eocene (Contreras et al., 2013). This is more consistent with the 4 × DYN simulation than the 2 × DYN simulation. Similarly, there is evidence that forests covered high Northern latitudes as well (Eberle and Greenwood, 2012), which is also most consistent with the 4 × DYN simulation. However, the predicted vegetation for the tropics is not particularly consistent with fossil evidence. There is evidence for paratropical or tropical forests (Willis and McElwain, 2002) across the majority of Africa and tropical regions of Asia and South America. However, TRIFFID predicts bare soil and grasses in both 2 × DYN and 4 × DYN for these regions.

3.2 Influence of dynamic vegetation on climate

3.2.1 Sea surface temperatures

Latitudinal SST gradients for simulations at 2 × and 4 × PI CO_2 are shown in Fig. 3. It can be seen that at low to mid latitudes, most model results are within the error bars of the SST proxy data. The RMS error, based on the SST data, is 12.8 °C for 2 × SHRUB, 11.4 °C for 4 × SHRUB, 12.7 °C for 2 × DYN and 10.6 °C for 4 × DYN. This shows that

CPD
9, 4705–4744, 2013

Investigating vegetation-climate feedbacks during the early Eocene

C. A. Loptson et al.

for both CO_2 levels, adding dynamic vegetation reduces the model-data discrepancy and that the mean SSTs are generally most consistent with 4 × DYN. However, there are uncertainties associated with the RMS error. The paucity and poor coverage of data means that this calculated value may not be representative of how well the model can reproduce the early Eocene climate. It can only be a broad indicator of how consistent the model is with the available data.

At high latitudes in the Northern Hemisphere the models predict temperatures over 20 °C cooler than proxy data. However, the uncertainty of this data point is rather large, spanning a range from 31 °C to 5 °C. Taking this into account, there is only a 5 °C discrepancy between the 4 × DYN results and data here. The 4 × SHRUB simulation had a discrepancy of 6 °C at this same grid point. This is the only data point for comparison in this region and more data would be required to reliably test the performance of the model in the Arctic.

3.2.2 Terrestrial temperatures

Figure 4 shows the zonal mean temperatures for each simulation and the terrestrial proxy data. Modelled Arctic temperatures are too cold and modelled tropical to mid latitude temperatures are similar to temperatures suggested by proxy data, which is consistent with the SST results. The RMS error, based on the surface air temperature data, is 16.0 °C for 2 × SHRUB, 11.7 °C for 4 × SHRUB, 14.6 °C for 2 × DYN and 9.5 °C for 4 × DYN. Again, the 4 × DYN shows the best agreement with proxy data. Changing vegetation distribution from SHRUB to DYN has the effect of increasing high latitude temperatures by approximately 1 °C, but this is insufficient to reproduce the very shallow temperature gradient indicated by available data in the high Northern latitudes.

Figure 5 shows annual mean surface air temperatures. The 2 × PI CO_2 simulations predict colder temperatures than the data suggests at every data point. All of the 4 × PI CO_2 simulations in general show good agreement with data in the low and mid latitudes, but the discrepancies increase with latitude and are largest in the Arctic.

CPD
9, 4705–4744, 2013

Table 2 summarises the global mean annual surface air temperatures (SATs) for all early Eocene experiments. It can be seen from this that vegetation feedbacks have a larger influence on temperature at higher CO_2 concentrations, as including dynamic vegetation results in a larger temperature increase at 4 × CO_2 (1.9 °C) than at 2 × CO_2 (1.1 °C).

3.3 Climate sensitivity

The results from this set of simulations can also be used to investigate how climate sensitivity changes when dynamic vegetation is included in the model. Climate sensitivity is defined as the global equilibrium temperature change in response to a doubling of atmospheric CO_2.

The climate sensitivity measured with fixed vegetation only takes into account relatively short term feedbacks and is sometimes called Charney sensitivity (Lunt et al., 2010b). Earth System Sensitivity (ESS) is defined by Lunt et al. (2010b) as the climate response when long-term feedbacks are included in addition to short-term feedbacks. By adding TRIFFID, which incorporates vegetation feedbacks, a closer estimation of the ESS can be made.

Figure 6 shows the global mean surface air temperatures for all five simulations. In these simulations, the climate sensitivity increases from 3.8 °C to 4.8 °C when dynamic vegetation is added. It would be expected that the climate sensitivity would be higher when vegetation feedbacks are incorporated into the model because vegetation feedbacks (e.g. albedo and hydrological) tend to be positive (Liu et al., 2006).

When vegetation is fixed at the output of 2 × DYN, but CO_2 is doubled to 4 × PI CO_2, the resulting mean global annual SAT increase is 3.3 °C. This is a lower climate sensitivity than for the SHRUB and DYN simulations.

It is possible to use these mean annual temperatures (MATs) and corresponding CO_2 levels to calculate the CO_2 concentrations that would produce temperatures most consistent with proxy data (i.e. the CO_2 level where the mean error is minimised). The "ideal" CO_2 concentrations vary depending on whether the marine or terrestrial datasets are used. For the terrestrial results, the ideal CO_2 values are calculated as 1720 ppm for the DYN simulations and 2550 ppm for the SHRUB simulations. Sea surface temperatures give ideal CO_2 concentrations of 1760 ppm for DYN and 2610 ppm for SHRUB. These predicted atmospheric CO_2 values are all in accord with the range of CO_2 estimates from proxies (Beerling and Royer, 2011; Lowenstein and Demicco, 2006; Pagani et al., 2009; Sluijs et al., 2006; Pearson et al., 2007). The "ideal" CO_2 values for the SHRUB simulations differ slightly from those calculated in the EoMIP study (Lunt et al., 2012), which predicts values of 2850 ppm based on terrestrial data and 2540 ppm based on SST data for the HadCM3L model. These differences can be attributed to the change in land surface scheme. The global annual mean SAT difference between the simulations with MOSES 2.1 and MOSES 2.2 is larger at higher CO_2 concentrations, resulting in a higher climate sensitivity in the SHRUB simulations than the EoMIP HadCM3L simulations.

The model is unstable at CO_2 levels this high with early Eocene boundary conditions, so it is not possible to test if the model is able to produce results consistent with data at these CO_2 levels.

Figure 7 shows how the temperature changes when CO_2 is doubled from 2 × to 4 × PI CO_2 in the SHRUB and DYN scenarios. This overall temperature increase is greater for the DYN simulations than the SHRUB simulations. This means that relative to SHRUB, DYN simulations show a greater decrease in sea ice extent at high latitudes when CO_2 is doubled to 4 × PI concentrations. The resulting ice-albedo feedbacks enhance warming at high latitudes resulting in the much greater polar amplification in the DYN scenario.

3.4 Separating effects of CO_2 and vegetation on climate

Figure 8a shows the effects of CO_2 alone on annual surface air temperature. This was calculated by taking the difference between simulations 2 × DYN and FIXED. Both simulations have the same vegetation distribution, fixed at that of the 2 × DYN simulation, so the only difference between them is the atmospheric CO_2 concentration.

CPD
9, 4705–4744, 2013

It can be seen that the temperature changes are highly dependent on region. The largest temperature increases due to CO_2 doubling is in the Arctic, where the global annual mean temperature increase is 8 °C and the Western Pacific, which sees a warming above 10 °C. However, there are some areas where less than 1 °C of warming occurs, such as some parts of the Pacific Ocean.

Changes in temperature due to vegetation changes between 2 × DYN and 4 × DYN are shown in Fig. 8b. These vegetation changes account for a global annual average temperature increase of 1.3 °C. However, they do not result in warming everywhere on a regional scale. A small decrease (∼1 °C) in temperature can be seen over some regions of land in the mid latitudes of the Northern Hemisphere, specifically over North America and Asia. In the Southern Hemisphere, the temperature increase is as much as 5 °C, which is similar in magnitude to the warming in these same regions when CO_2 is doubled. The areas of highest temperature increase in the tropics correlate with the areas of increased bare soil coverage (see Figs. 1 and 2).

3.5 Seasonality

The influence of CO_2 and vegetation on climate are dependent on the season. Figures 9 and 10 show how these factors change the surface air temperature in the Northern Hemisphere summer months (JJA) and in the winter months (DJF). Global mean surface air temperatures are shown in Table 2.

Vegetation changes alone result in a global average temperature increase of 1.7 °C in DJF and 1.6 °C in JJA. Doubling CO_2 alone results in global average temperature increases of 3.6 °C in DJF and 3.4 °C in JJA, more than twice as large as the impact of vegetation changes.

Figure 9 shows that doubling CO_2 without changing vegetation has the largest effect on temperature in the Arctic in DJF, where the temperature increase of more than 15 °C in some areas. This is due to a decrease in winter sea ice cover (as a result of warming due to increased CO_2) and associated albedo-ice feedbacks. This is also the mechanism behind the large temperature increase in some regions off the coast of Antarctica in JJA, but the change is smaller in magnitude and area than the Arctic.

In addition, a temperature increase of 8–9 °C is seen in the mid latitudes of the Northern Hemisphere in JJA. This is a result of increased atmospheric water vapour and differences in albedo due to changes in cloud cover. These changes are most likely associated with enhanced vegetation feedbacks as a result of higher atmospheric CO_2 concentrations.

Vegetation has the greatest effect on temperature over terrestrial equatorial regions in JJA, and at high latitudes in DJF (Fig. 10). Although vegetation changes result in a temperature increase when looking at the global mean, these vegetation differences result in a slight cooling effect in the mid latitudes of the Northern Hemisphere, especially in summer. This is due to a combination of differences in surface albedo, where broadleaf trees replace needleleaf trees, and albedo due to changes in clouds.

Figure 11 shows the effect of dynamic vegetation on surface air temperature increase when CO_2 is doubled, i.e. (4 × DYN – 2 × DYN) – (4 × SHRUB – 2 × SHRUB), in JJA and DJF. These figures show that the strongest differences in seasonal climate at high latitudes in DJF.

The Arctic shows a large temperature difference in DJF, but not in JJA. This is a result of ice-albedo feedbacks that occur due to a larger reduction in winter sea ice when CO_2 is doubled with dynamic vegetation compared to homogeneous shrubs.

There is no evidence for any sea ice in the early Eocene, however it is present in our model. This is just a consequence of temperatures being too low at high latitudes. If the temperatures at high latitudes matched those indicated by proxy data, then it is likely seasonality would be reduced due to a lack of sea ice.

In the Southern Hemisphere, the largest warming also occurs in DJF, i.e. austral summer. This is when plants would be most productive and therefore when associated water vapour feedbacks would be strongest. In addition, there is no incoming solar radiation over Antarctica in JJA, so changes in albedo would have no effect on temperature in these months but would have an effect in DJF.

CPD
9, 4705–4744, 2013

3.6 Precipitation differences

Vegetation affects the hydrological cycle, so it would be expected that adding dynamic vegetation will affect precipitation distributions and magnitudes. Annual global means for precipitation are shown in Table 2.

Adding dynamic vegetation to the simulations does enhance the hydrological cycle. Compared to the shrub simulations, the simulations with TRIFFID have precipitation rates 4.9 % higher at 2 × and 6.3 % higher at 4 × PI CO_2 .

Increasing CO_2 also increases total annual precipitation for a given vegetation scheme. When atmospheric CO_2 concentrations are increased from 2 × to 4 ×, global mean rainfall rates increase by 4.6 % with fixed homogeneous shrubs (Fig. 12a) and 5.9 % in the simulations where TRIFFID is included (Fig. 12b). By comparison with the FIXED simulation, it can be seen that this increase in total precipitation between 2 × DYN and 4 × DYN is mostly due to the change in climate rather than the change in vegetation.

When dynamic vegetation is included in the model, the band of enhanced precipitation across the equatorial Pacific Ocean covers a larger area relative to the simulations with homogeneous shrubs.

However, precipitation rates show a large percentage decrease (up to 100 %) in the South Atlantic Ocean when TRIFFID is included in the model. This is much larger than the simulations with fixed shrubs, which sees a decrease of around 20 % in this same region.

The areas over land where there is a decrease of 20 to 40 % in precipitation in Fig. 12b correlate with areas of bare soil in the 4 × DYN simulation. Areas of percentage decrease in precipitation are also associated with areas where shrubs replace trees as the dominant PFT around areas of bare soil.

The percentage increases in precipitation rates at high latitudes are enhanced slightly in the simulations with TRIFFID compared with the SHRUB simulations.

CPD
9, 4705–4744, 2013

3.7 Energy balance analysis

Traditionally it has been difficult to diagnose which processes are responsible for the differences in surface air temperature between two different simulations. Lunt et al. (2012) have included additional diagnostics to the 1 dimensional energy balance analysis detailed in Heinemann et al. (2009) to show the extent to which changes in five different aspects of the planet and atmosphere (heat transport, emissivity due to clouds, emissivity due to greenhouse gases, albedo of clouds and albedo of planetary surface) contribute to the overall temperature difference between GCM simulations. The full details of the energy balance calculations used here can be found in Lunt et al. (2012).

It should be noted that the temperature difference due to changes in albedo of planetary surface also include changes in atmospheric effects (i.e. how much radiation is scattered by the atmosphere). However, this only needs to be taken into account when the thickness of the atmosphere or orographic height at a gridpoint varies between simulations (e.g. comparing a pre-industrial simulation with an early Eocene simulation). This is not the case in these comparisons, so the difference in atmospheric effects is negligible.

Energy balance analysis shows that the climate sensitivity is lower for the FIXED simulations than the SHRUB simulations mainly due to GHG forcing, resulting in 0.3 °C less warming. The differences in planetary surface albedo between 2 × and 4 × result in 0.1 °C less warming in the FIXED case compared to the SHRUB simulations. The emissivity due to clouds is also different in the FIXED and SHRUB cases. It acts to cool the climate for both vegetation distributions but has a lesser cooling effect when CO_2 is doubled in the SHRUB case.

The two dimensional energy balance analysis for a doubling of CO_2 from 2 × to 4 × PI CO_2 is shown in Fig. 13 and Table 3 summarises the one dimensional energy balance analysis results. Figure 13a is for the homogeneous shrub case, and so excludes

CPD
9, 4705–4744, 2013

vegetation feedbacks, whereas Fig. 13b shows the different contributions to the temperature change when vegetation feedbacks are included.

In both of these cases, emissivity due to greenhouse gases is the largest contributing factor to the overall temperature increase. However, the contribution is 0.7 °C larger for the simulation with interactive vegetation compared to fixed uniform vegetation. Since the change in CO_2 is the same in both cases, it means that there is a higher concentration of another greenhouse gas in the atmosphere (water vapour) when HadCM3L is coupled to TRIFFID.

When CO_2 is doubled, the increase in total evaporation is over 50 % larger for the dynamic vegetation simulations and specific humidity is higher than when the land surface is covered with shrubs only. This a result of higher temperatures in the DYN simulations and hydrological recycling due to vegetation. In addition, the DYN simulations also show reduced subsurface runoff compared to the SHRUB simulations, which may be due to the root systems of some PFTs being more effective at retaining water. These hydrological feedbacks may be driven by the change in surface albedo due to the altered vegetation distribution.

In both Fig 13a) and b, the polar amplification of warming is apparent. The high latitudes increase in temperature more than the equator by 3 °C and 4 °C respectively. The surface and atmospheric albedo effect becomes more important in Antarctica for the DYN simulations, with 2 °C more warming at the highest Southern latitudes compared to the SHRUB simulations. Changes in cloud albedo result in a larger temperature increase in the low latitudes in the DYN simulations and also make a larger (i.e. less negative) contribution to total temperature change in the Arctic. Heat transport to the high latitudes is reduced in the DYN simulations compared to the SHRUB simulations. This result is consistent with other studies, e.g. Sagoo et al. (2013), that have found a reduction in ocean heat transport as tropical SSTs increase.

Figure 13c and d show the change in temperature when TRIFFID is coupled to the GCM, compared with prescribed homogeneous shrubs covering all land. It can be seen that as CO_2 increases, the vegetation distribution has a larger effect on temperature.

CPD
9, 4705–4744, 2013

At $4 \times$ PI CO_2, the overall temperature increase is almost double that of the $2 \times$ PI CO_2 simulations. This is due to an increase in GHG and cloud albedo effects. The temperature increase due to GHGs more than doubling between Fig. 13c and d. This is consistent with water vapour feedbacks becoming enhanced as CO_2 concentrations increase.

The change in vegetation distribution has a much larger effect in Antarctica at $4 \times CO_2$ compared to $2 \times CO_2$. This is mainly due to a 2 °C temperature increase in the contribution of surface albedo and water vapour. This is consistent with the differences in predicted vegetation distributions; the $2 \times$ DYN simulation still has quite high coverage of shrubs on Antarctica, whereas broadleaf trees dominate almost the entire continent in $4 \times$ DYN. The effect of albedo due to clouds seems to be amplified in the tropics in for $4 \times CO_2$ relative to $2 \times CO_2$ and is responsible for ~ 1 °C warming at the highest Northern latitudes.

4 Conclusions

This paper has investigated how the vegetation distributions predicted by TRIFFID vary with atmospheric CO_2, and how these changes in vegetation affect the climate and climate sensitivity. It has also investigated the reasons behind the temperature differences between simulations using an energy balance model.

The strongest warming when CO_2 is doubled is seen in the Arctic and is due to ice-albedo feedbacks. These feedbacks are stronger with dynamic vegetation than with shrubs everywhere, as the vegetation feedbacks enhance initial warming which triggers more ice melt.

Dynamic vegetation enhances the hydrological cycle, which is consistent with previous studies, e.g. Liu et al. (2006). The DYN simulations have higher precipitation rates than SHRUB for a given atmospheric CO_2 level and show a larger increase when CO_2 is doubled.

CPD
9, 4705–4744, 2013

Including a dynamic vegetation component to the model increases global temperatures, mainly through water vapour feedbacks, and goes some way to resolving the model-data discrepancies. The 4 × DYN simulation is most consistent with data, in terms of both predicted vegetation and modelled temperatures. However, model-data discrepancies still exist, especially at high latitudes, for all model scenarios described here. The modelled latitudinal temperature gradient is too steep, with high latitudes not reaching the warmth predicted by proxy data. The paucity of data, especially in the Arctic and Antarctica, makes it challenging to discern the extent of the model-data discrepancies at high latitudes. However, it can be concluded that vegetation feedbacks alone are not enough to explain the model-data temperature mismatch. There could be processes that are poorly represented or not present in the model and/or with data (e.g. seasonal bias, high latitude clouds).

The DYN simulations have a smaller RMS error than the SHRUB simulations for a given CO_2 level when compared with temperatures inferred from proxy data. As a result of the higher temperatures and climate sensitivity in the DYN simulations, they also have a lower "ideal" CO_2 value. This means that vegetation feedbacks can explain, to some extent, how the early Eocene warmth could be consistent with atmospheric CO_2 levels at the lower end of the estimated range (Beerling and Royer, 2011; Lowenstein and Demicco, 2006; Pagani et al., 2009; Sluijs et al., 2006; Pearson et al., 2007).

In future simulations, TRIFFID should be adapted to be more appropriate for the early Eocene. This could be done by replacing C_4 with a vegetation type that is known to exist in this time period, such as ferns. In addition, parameters of other PFTs within TRIFFID could be adjusted to be more consistent with paleovegetation, as the model currently uses modern day parameter values and it is possible that these values have changed over time. This would give a more realistic vegetation representation for the modelled early Eocene climate and also allow a more accurate comparison between model results and data.

CPD
9, 4705–4744, 2013

Acknowledgements. This work was funded by a NERC grant and is part of the PALEOPOLAR project within the "Co-Evolution of Life and the Planet" programme.

References

Beerling, D. J. and Royer, D. L.: Convergent Cenozoic CO_2 history, Nat. Geosci., 4, 418–420, 2011. 4707, 4716, 4723

Beerling, D. J., Fox, A., Stevenson, D. S., and Valdes, P. J.: Enhanced chemistry-climate feedbacks in past greenhouse worlds, P. Natl. Acad. Sci., 2011. 4707

Bijl, P. K., Schouten, S., Sluijs, A., Reichart, G., Zachos, J. C., and Brinkhuis, H.: Early Palaeogene temperature evolution of the southwest Pacific Ocean, Nature, 461, 776–779, 2009. 4707

Bonan, G. B.: Forests and Climate Change: Forcings, Feedbacks, and the Climate Benefits of Forests, Science, 320, 1444–1449, 2008. 4709

Christin, P.-A., Osborne, C. P., Sage, R. F., Arakaki, M., and Edwards, E. J.: C4 eudicots are not younger than C4 monocots, J. Exp. Bot., 62, 3171–3181, 2011. 4711

Collins, W. D., Rasch, P. J., Boville, B. A., Hack, J. J., McCaa, J. R., Williamson, D. L., Briegleb, B. P., Bitz, C. M., Lin, S.-J., and Zhang, M.: The Formulation and Atmospheric Simulation of the Community Atmosphere Model Version 3 (CAM3), J. Climate, 19, 2144–2161, 2006. 4708

Contreras, L., Pross, J., Bijl, P. K., Koutsodendris, A., Raine, J. I., van de Schootbrugge, B., and Brinkhuis, H.: Early to Middle Eocene vegetation dynamics at the Wilkes Land Margin (Antarctica), Rev. Palaeobot. Palyno., 197, 119–142, 2013. 4710, 4713

Cox, P.: Description of the "TRIFFID" Dynamic Global Vegetation Model, Tech. Rep. Hadley Centre Technical Note 24, Meteorological Office, Bracknell, Berkshire, 2001. 4711

Donnadieu, Y., Goddéris, Y., and Bouttes, N.: Exploring the climatic impact of the continental vegetation on the Mezosoic atmospheric CO_2 and climate history, Clim. Past, 5, 85–96, doi:10.5194/cp-5-85-2009, 2009. 4712

Eberle, J. J. and Greenwood, D. R.: Life at the top of the greenhouse Eocene world – A review of the Eocene flora and vertebrate fauna from Canada's High Arctic, Geol. Soc. Am. Bull., 124, 3–23, 2012. 4713

Eberle, J. J., Fricke, H. C., Humphrey, J. D., Hackett, L., Newbrey, M. G., and Hutchison, J. H.: Seasonal variability in Arctic temperatures during early Eocene time, Earth Planet. Sc. Lett., 296, 481–486, 2010. 4709

Edwards, E. J., Osborne, C. P., Strömberg, C. A. E., Smith, S. A., and Consortium, C. G.: The Origins of C4 Grasslands: Integrating Evolutionary and Ecosystem Science, Science, 328, 587–591, 2010. 4711

Essery, R., Best, M., and Cox, P.: MOSES 2.2 Technical Documentation, Hadley Centre technical note 30, 2001. 4711

Francis, J. and Poole, I.: Cretaceous and early Tertiary climates of Antarctica: evidence from fossil wood, Palaeogeogr. Palaeocl., 182, 47–64, 2002. 4713

Gordon, C., Cooper, C., Senior, C. A., Banks, H., Gregory, J. M., Johns, T. C., Mitchell, J. F. B., and Wood, R. A.: The simulation of SST, sea ice extents and ocean heat transports in a version of the Hadley Centre coupled model without flux adjustments, Clim. Dynam., 16, 147–168, 2000. 4708

Heinemann, M., Jungclaus, J. H., and Marotzke, J.: Warm Paleocene/Eocene climate as simulated in ECHAM5/MPI-OM, Clim. Past, 5, 785–802, doi:10.5194/cp-5-785-2009, 2009. 4707, 4720

Hollis, C. J., Taylor, K. W. R., Handley, L., Pancost, R. D., Huber, M., Creech, J. B., Hines, B. R., Crouch, E. M., Morgans, H. E. G., Crampton, J. S., Gibbs, S., Pearson, P. N., and Zachos, J. C.: Early Paleogene temperature history of the Southwest Pacific Ocean: Reconciling proxies and models, Earth Planet. Sc. Lett., 349–350, 53–66, 2012. 4710

Huber, M.: A Hotter Greenhouse?, Science, 321, 353–354, 2008. 4708

Huber, M. and Caballero, R.: The early Eocene equable climate problem revisited, Clim. Past, 7, 603–633, doi:10.5194/cp-7-603-2011, 2011. 4707, 4735, 4736

Jaramillo, C., Ochoa, D., Contreras, L., Pagani, M., Carvajal-Ortiz, H., Pratt, L. M., Krishnan, S., Cardona, A., Romero, M., Quiroz, L., Rodriguez, G., Rueda, M. J., de la Parra, F., Morón, S., Green, W., Bayona, G., Montes, C., Quintero, O., Ramirez, R., Mora, G., Schouten, S., Bermudez, H., Navarrete, R., Parra, F., Alvarán, M., Osorno, J., Crowley, J. L., Valencia, V., and Vervoort, J.: Effects of Rapid Global Warming at the Paleocene-Eocene Boundary on Neotropical Vegetation, Science, 330, 957–961, 2010. 4708

Kiehl, J. and Shields, C.: Sensitivity of the paleocene-eocene thermal maximum climate to cloud properties, Philos. T. R. Soc. A., in press, 2013. 4708

Kim, J.-H., van der Meer, J., Schouten, S., Helmke, P., Willmott, V., Sangiorgi, F., Koç, N., Hopmans, E. C., and Damsté, J. S. S.: New indices and calibrations derived from the distribution of crenarchaeal isoprenoid tetraether lipids: Implications for past sea surface temperature reconstructions, Geochim. Cosmochim. Ac., 74, 4639–4654, 2010. 4710

Kump, L. R. and Pollard, D.: Amplification of cretaceous warmth by biological cloud feedbacks, Science, 320, p. 195, 2008. 4708

Liu, Z., Notaro, M., Kutzbach, J., and Liu, N.: Assessing Global Vegetation–Climate Feedbacks from Observations, J. Climate, 19, 787–814, 2006. 4715, 4722

Liu, Z., Pagani, M., Zinniker, D., DeConto, R., Huber, M., Brinkhuis, H., Shah, S. R., Leckie, R. M., and Pearson, A.: Global cooling during the eocene-oligocene climate transition, Science, 323, 1187–1190, 2009. 4710

Lowenstein, T. K. and Demicco, R. V.: Elevated Eocene atmospheric CO_2 and its subsequent decline, Science, 313, p. 1928, 2006. 4707, 4716, 4723

Lunt, D., Valdes, P., Dunkley Jones, T., Ridgwell, A., Haywood, A., Schmidt, D., Marsh, R., and Maslin, M.: CO_2-driven ocean circulation changes as an amplifier of Paleocene-Eocene thermal maximum hydrate destabilization, Geology, 38, 875–878, 2010a. 4711, 4712

Lunt, D. J., Haywood, A. M., Schmidt, G. A., Salzmann, U., Valdes, P. J., and Dowsett, H. J.: Earth system sensitivity inferred from Pliocene modelling and data, Nat. Geosci., 3, 60–64, 2010b. 4711, 4715

Lunt, D. J., Dunkley Jones, T., Heinemann, M., Huber, M., LeGrande, A., Winguth, A., Loptson, C., Marotzke, J., Roberts, C. D., Tindall, J., Valdes, P., and Winguth, C.: A model-data comparison for a multi-model ensemble of early Eocene atmosphere-ocean simulations: EoMIP, Clim. Past, 8, 1717–1736, doi:10.5194/cp-8-1717-2012, 2012. 4708, 4710, 4711, 4716, 4720, 4734

Markwick, P. and Valdes, P.: Palaeo-digital elevation models for use as boundary conditions in coupled ocean-atmosphere GCM experiments: a Maastrichtian (late Cretaceous) example, Palaeogeogr. Palaeocl., 213, 37–63, 2004. 4711

Martin, P. A., Lea, D. W., Rosenthal, Y., Shackleton, N. J., Sarnthein, M., and Papenfuss, T.: Quaternary deep sea temperature histories derived from benthic foraminiferal Mg/Ca, Earth Planet Sc. Lett., 198, 193–209, 2002. 4707

Otto-Bliesner, B. and Upchurch, G.: Vegetation-induced warming of high-latitude regions during the late Cretaceous period, Nature, 385, 804–807, 1997. 4708

Pagani, M., Caldeira, K., Berner, R., and Beerling, D. J.: The role of terrestrial plants in limiting atmospheric CO_2 decline over the past 24[thinsp]million years, Nature, 460, 85–88, 2009. 4707, 4716, 4723

Pearson, P. N., van Dongen, B. E., Nicholas, C. J., Pancost, R. D., Schouten, S., Singano, J. M., and Wade, B. S.: Stable warm tropical climate through the Eocene Epoch, Geology, 35, 211–214, 2007. 4707, 4708, 4709, 4716, 4723

Pope, V. D., Gallani, M. L., Rowntree, P. R., and Stratton, R. A.: The impact of new physical parameterisations in the Hadley Centre Climate Model: HadAM3, Clim. Dynam., 16, 123–146, 2000. 4708

Pross, J., Contreras, L., Bijl, P. K., Greenwood, D. R., Bohaty, S. M., Schouten, S., Bendle, J. A., Rohl, U., Tauxe, L., Raine, J. I., Huck, C. E., van de Flierdt, T., Jamieson, S. S. R., Stickley, C. E., van de Schootbrugge, B., Escutia, C., and Brinkhuis, H.: Persistent near-tropical warmth on the Antarctic continent during the early Eocene epoch, Nature, 488, 73–77, 2012. 4735, 4736

Roberts, C. D., LeGrande, A. N., and Tripati, A. K.: Climate sensitivity to Arctic seaway restriction during the early Paleogene, Earth Planet. Sc. Lett., 286, 576–585, 2009. 4707, 4709

Sagoo, N., Valdes, P., Flecker, R., and Gregoire, L.: The early eocene equable climate problem: Can perturbations of climate model parameters identify possible solutions?, Philos. T. R. Soc. A., in press, 2013. 4708, 4721

Sewall, J. O., Sloan, L. C., Huber, M., and Wing, S.: Climate sensitivity to changes in land surface characteristics, Global Planet. Change, 26, 445–465, 2000. 4709

Shellito, C. J., Lamarque, J.-F., and Sloan, L. C.: Early Eocene Arctic climate sensitivity to $p$$CO_2$ and basin geography, Geophys. Res. Lett., 36, L09707, doi:10.1029/2009GL037248, 2009. 4707

Sloan, L. C. and Morrill, C.: Orbital forcing and Eocene continental temperatures, Palaeogeogr. Palaeocl., 144, 21–35, 1998. 4707

Sloan, L. and Pollard, D.: Polar stratospheric clouds: A high latitude warming mechanism in an ancient greenhouse world, Geophys. Res. Lett., 25, 3517–3520, 1998. 4708

Sluijs, A., Schouten, S., Pagani, M., Woltering, M., Brinkhuis, H., Damsté, J. S. S., Dickens, G. R., Huber, M., Reichart, G.-J., Stein, R., Matthiessen, J., Lourens, L. J., Pedentchouk, N., Backman, J., Moran, K., and the Expedition 302 Scientists: Subtropical Arctic Ocean temperatures during the Palaeocene/Eocene thermal maximum, Nature, 441, 610–613, 2006. 4707, 4716, 4723

Sluijs, A., Röhl, U., Schouten, S., Brumsack, H.-J., Sangiorgi, F., Sinninghe Damsté, J. S., and Brinkhuis, H.: Arctic late Paleocene-early Eocene paleoenvironments with special emphasis on the Paleocene-Eocene thermal maximum (Lomonosov Ridge, Integrated Ocean Drilling Program Expedition 302), Paleoceanography, 23, PA1S11, doi:10.1029/2007PA001495, 2008. 4707

Tindall, J., Flecker, R., Valdes, P., Schmidt, D. N., Markwick, P., and Harris, J.: Modelling the oxygen isotope distribution of ancient seawater using a coupled ocean-atmosphere GCM: Implications for reconstructing early Eocene climate, Earth Planet. Sc. Lett., 292, 265–273, 2010. 4711

Vicentini, A., Barber, J. C., Aliscioni, S. S., Giussani, L. M., and Kellogg, E. A.: The age of the grasses and clusters of origins of C4 photosynthesis, Global Change Biol., 14, 2963–2977, 2008. 4711

Willis, K. and McElwain, J.: The Evolution of Plants, Oxford University Press, 2002. 4713

Winguth, A., Shellito, C., Shields, C., and Winguth, C.: Climate Response at the Paleocene–Eocene Thermal Maximum to Greenhouse Gas Forcing – A Model Study with CCSM3, J. Climate, 23, 2562–2584, 2010. 4707

Wolfe, A. P., Csank, A. Z., Reyes, A. V., McKellar, R. C., Tappert, R., and Muehlenbachs, K.: Pristine Early Eocene Wood Buried Deeply in Kimberlite from Northern Canada, PlOS One, 7, e45537, doi:10.1371/journal.pone.0045537, 2012. 4735, 4736

Zachos, J., Pagani, M., Sloan, L., Thomas, E., and Billups, K.: Trends, Rhythms, and Aberrations in Global Climate 65 Ma to Present, Science, 292, 686–693, 2001. 4707

Zachos, J. C., Schouten, S., Bohaty, S., Quattlebaum, T., Sluijs, A., Brinkhuis, H., Gibbs, S. J., and Bralower, T. J.: Extreme warming of mid-latitude coastal ocean during the Paleocene-Eocene Thermal Maximum: Inferences from TEX86 and isotope data, Geology, 34, 737–740, 2006. 4707

Zhou, J., Poulsen, C. J., Rosenbloom, N., Shields, C., and Briegleb, B.: Vegetation-climate interactions in the warm mid-Cretaceous, Clim. Past, 8, 565–576, doi:10.5194/cp-8-565-2012, 2012. 4709

CPD
9, 4705–4744, 2013

Investigating vegetation-climate feedbacks during the early Eocene

C. A. Loptson et al.

Title Page
Abstract | Introduction
Conclusions | References
Tables | Figures
◀◀ | ▶▶
◀ | ▶
Back | Close
Full Screen / Esc
Printer-friendly Version
Interactive Discussion

Table 1. Summary of all Eocene model simulations.

Experiment name	CO_2 level	Vegetation
2 × SHRUB	2	Fixed (homogeneous shrubland)
4 × SHRUB	4	Fixed (homogeneous shrubland)
2 × DYN	2	Dynamic (predicted by TRIFFID)
4 × DYN	4	Dynamic (predicted by TRIFFID)
FIXED	4	Fixed (vegetation distribution of 2 × DYN)

CPD
9, 4705–4744, 2013

Table 2. Table showing climatological means for all Eocene experiments.

Experiment name	Precipitation (mm day^{-1})	Global mean SAT (°C)		
		Annual	DJF	JJA
2 × SHRUB	3.05	17.8	16.2	19.7
4 × SHRUB	3.19	21.7	20.2	23.7
2 × DYN	3.20	18.9	16.9	20.6
4 × DYN	3.39	23.6	22.0	25.6
FIXED	3.27	22.3	20.6	24.3

CPD
9, 4705–4744, 2013

Discussion Paper | Discussion Paper | Discussion Paper | Discussion Paper |

CPD

9, 4705–4744, 2013

Investigating vegetation-climate feedbacks during the early Eocene

C. A. Loptson et al.

Table 3. Summary of the 1 dimensional energy balance analysis. The total global MAT difference is denoted by ΔT, ΔT_{lwc} is the component of ΔT due to long-wave cloud changes (i.e. changes in emissivity due to clouds), ΔT_{gg} is the component due to greenhouse gases, ΔT_{swc} is the short-wave cloud contribution (i.e. changes in albedo due to clouds) and ΔT_{salb} is the contribution of planetary surface albedo changes. The contribution from each factor as a percentage of ΔT is shown in brackets. All temperatures are in degrees Celsius.

Experiment names	ΔT	ΔT_{lwc}	ΔT_{gg}	ΔT_{swc}	ΔT_{salb}
4 × SHRUB – 2 × SHRUB	3.8	−0.5 (−14.3 %)	3.5 (91.6 %)	0.7 (17.3 %)	0.3 (7.0 %)
4 × DYN – 2 × DYN	4.8	−0.6 (−11.8 %)	4.2 (87.2 %)	1.0 (20.2 %)	0.2 (4.8 %)
2 × DYN – 2 × SHRUB	1.1	−0.0 (−4.0 %)	0.5 (50.1 %)	0.1 (11.0 %)	0.5 (49.6 %)
4 × DYN – 4 × SHRUB	2.0	−0.1 (−2.9 %)	1.2 (59.6 %)	0.4 (21.1 %)	0.5 (23.8 %)

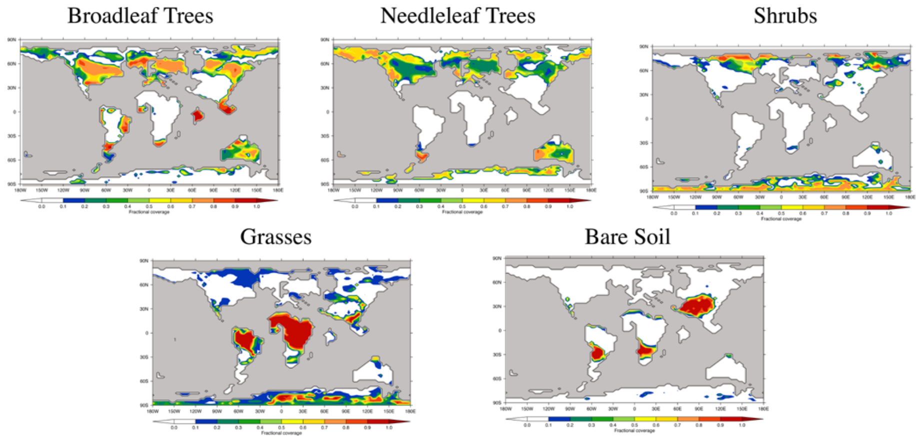

Fig. 1. Global early Eocene vegetation distributions for 2 × DYN as predicted by TRIFFID.

CPD
9, 4705–4744, 2013

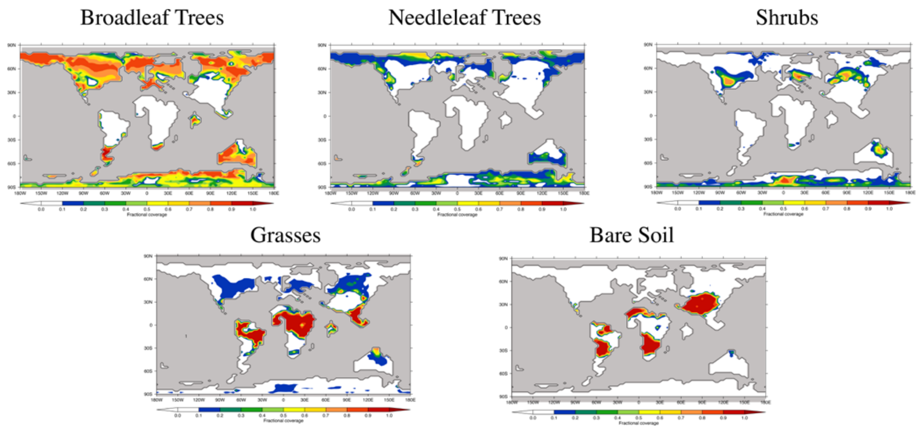

Fig. 2. Global early Eocene vegetation distributions for 4 × DYN as predicted by TRIFFID.

CPD
9, 4705–4744, 2013

Investigating vegetation-climate feedbacks during the early Eocene

C. A. Loptson et al.

Title Page
Abstract | Introduction
Conclusions | References
Tables | Figures
◂◂ | ▸▸
◂ | ▸
Back | Close
Full Screen / Esc
Printer-friendly Version
Interactive Discussion

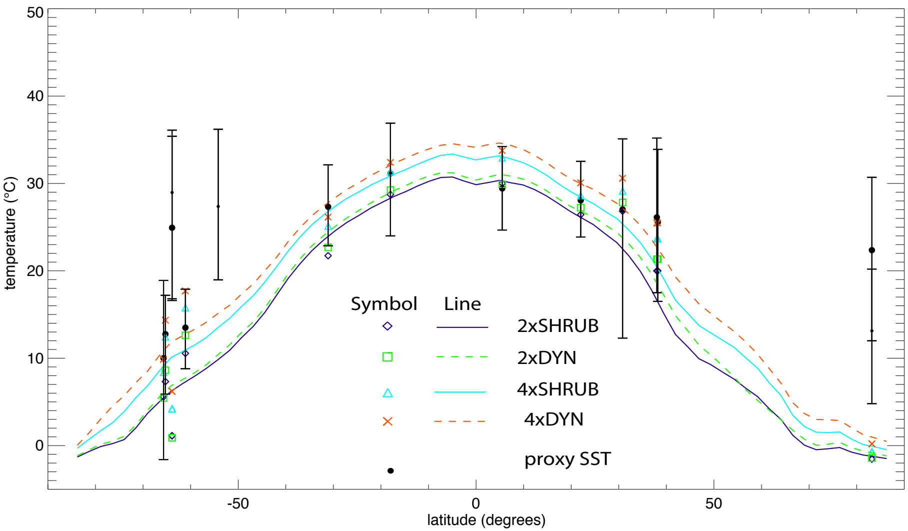

Fig. 3. Zonal mean annual SSTs for 2 × SHRUB (dark blue diamonds), 2 × DYN (green squares), 4×SHRUB (light blue triangles) and 4 × DYN (orange crosses). The black dots show the terrestrial temperatures indicated by proxy data with error bars (the smaller black dots indicate early Eocene climatic optimum temperatures). The coloured shapes show the temperature at the same latitude and longitude as the location of the data as predicted by each model. The lines show the modelled latitudinal temperature gradients for each simulation. Dataset from Lunt et al. (2012).

CPD
9, 4705–4744, 2013

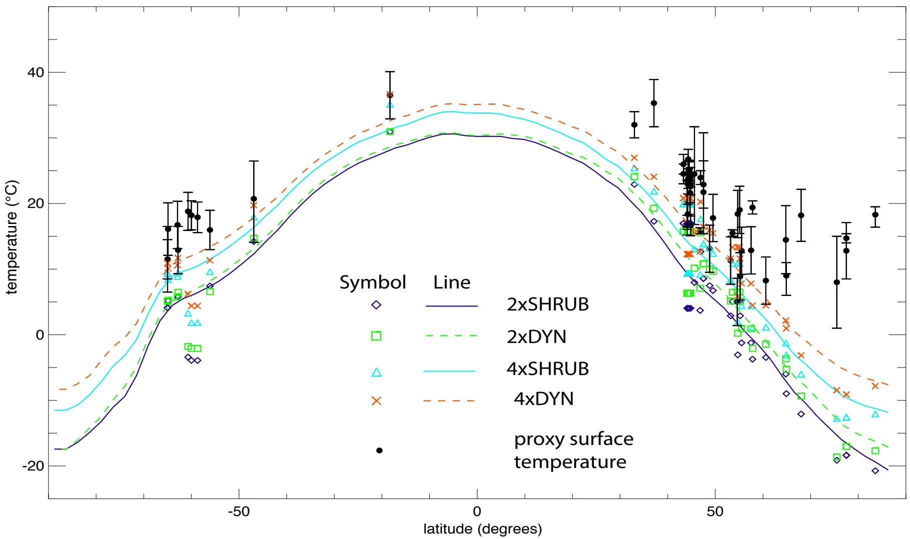

Fig. 4. As Fig. 3 but for zonal annual mean surface air temperatures. Dataset from Huber and Caballero (2011), Pross et al. (2012) and Wolfe et al. (2012).

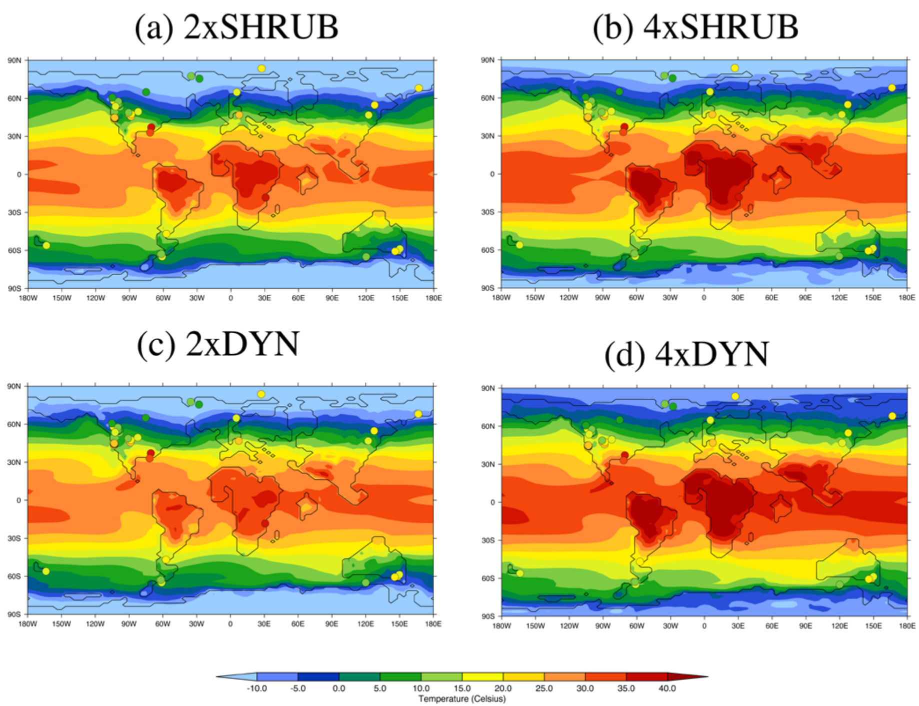

Fig. 5. Comparison of modelled global annual mean 2 m surface air temperature with temperatures inferred from proxy data. The circles show the temperature inferred from proxy data at the point where the data was collected. Dataset from Huber and Caballero (2011), Pross et al. (2012) and Wolfe et al. (2012).

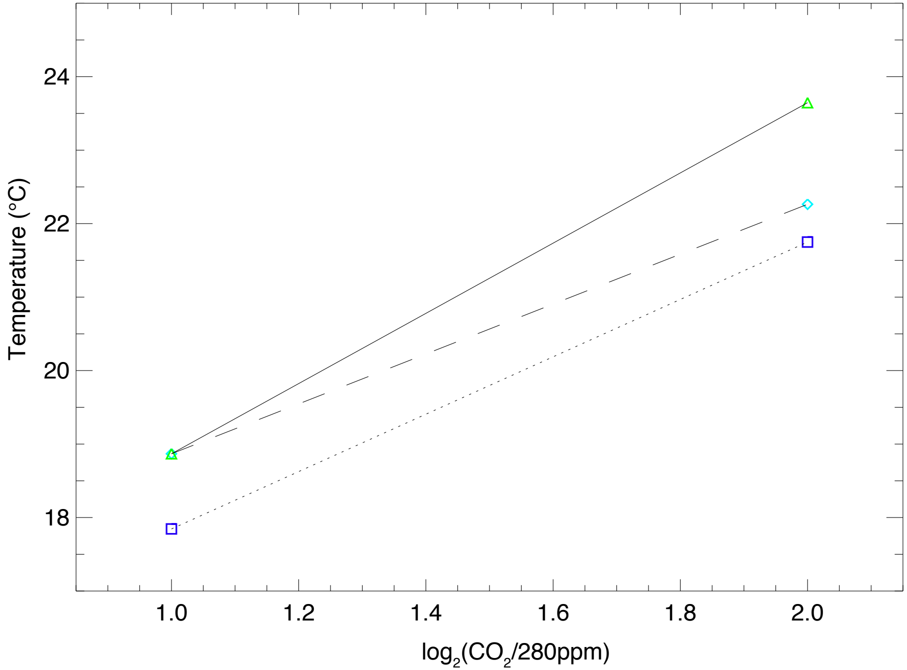

Fig. 6. Climate sensitivity measured by HadCM3L with dynamic vegetation (solid line), fixed homogeneous shrubs (dotted line) and fixed, non-homogeneous vegetation (dashed line).

CPD
9, 4705–4744, 2013

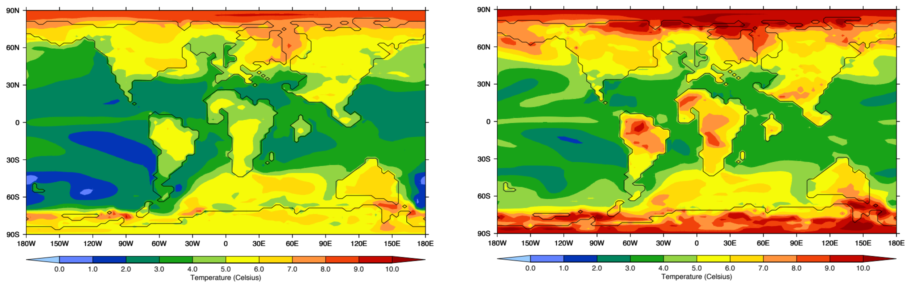

(a) (b)

Fig. 7. Annual surface air temperature difference between **(a)** 4 × SHRUB and 2 × SHRUB and **(b)** 4 × DYN and 2 × DYN.

CPD
9, 4705–4744, 2013

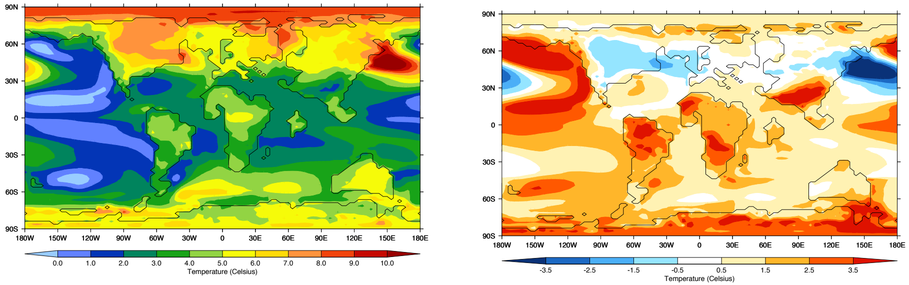

(a) (b)

Fig. 8. Difference in annual surface air temperature when **(a)** CO_2 is doubled but vegetation is fixed (FIXED – 2 × DYN) **(b)** and CO_2 is constant but vegetation distribution changes (4 × DYN – FIXED).

CPD
9, 4705–4744, 2013

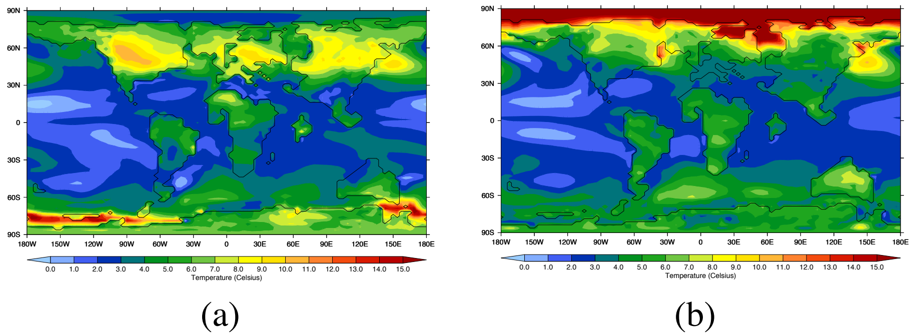

Fig. 9. Surface air temperature differences when CO_2 is doubled from 2 × to 4 × (i.e. FIXED – 2 × DYN) **(a)** in JJA and **(b)** in DJF

CPD
9, 4705–4744, 2013

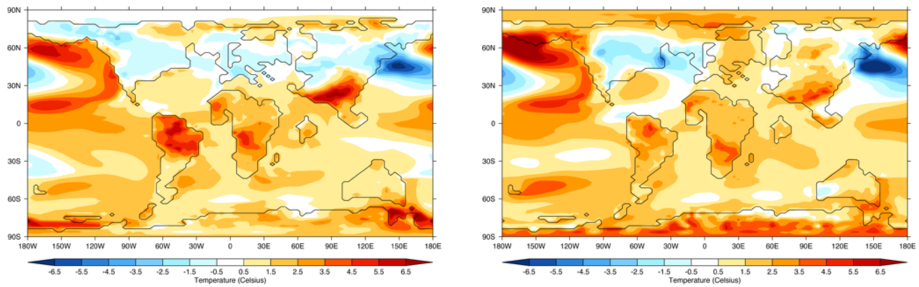

(a) (b)

Fig. 10. Surface air temperature differences when vegetation distribution is changed from that of 2 × DYN to 4 × DYN but with CO_2 constant at 4 × (i.e. 4 × DYN – FIXED) **(a)** in JJA and **(b)** in DJF.

CPD
9, 4705–4744, 2013

CPD
9, 4705–4744, 2013

Investigating vegetation-climate feedbacks during the early Eocene

C. A. Loptson et al.

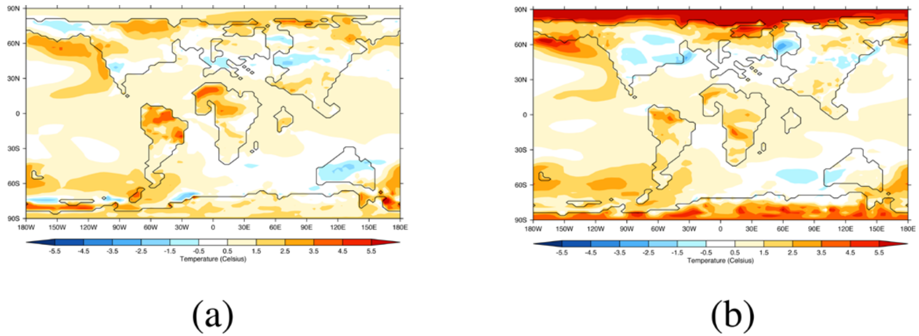

Fig. 11. The effect of dynamic vegetation on the surface air temperature increase when CO_2 is doubled **(a)** in JJA and **(b)** in DJF.

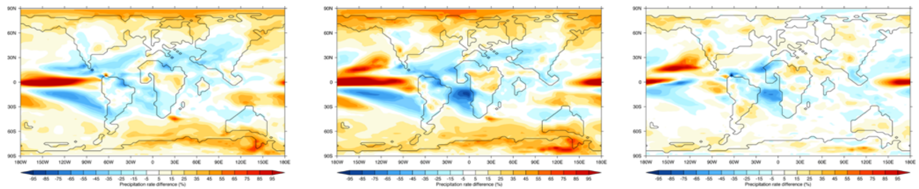

(a) (b) (c)

Fig. 12. Percentage change in annual precipitation between **(a)** 4 × SHRUB and 2 × SHRUB, **(b)** 4 × DYN and 2 × DYN, and **(c)** shows the effect of dynamic vegetation on the precipitation difference when CO_2 is doubled, i.e. the difference between figures **(a)** and **(b)**.

CPD
9, 4705–4744, 2013

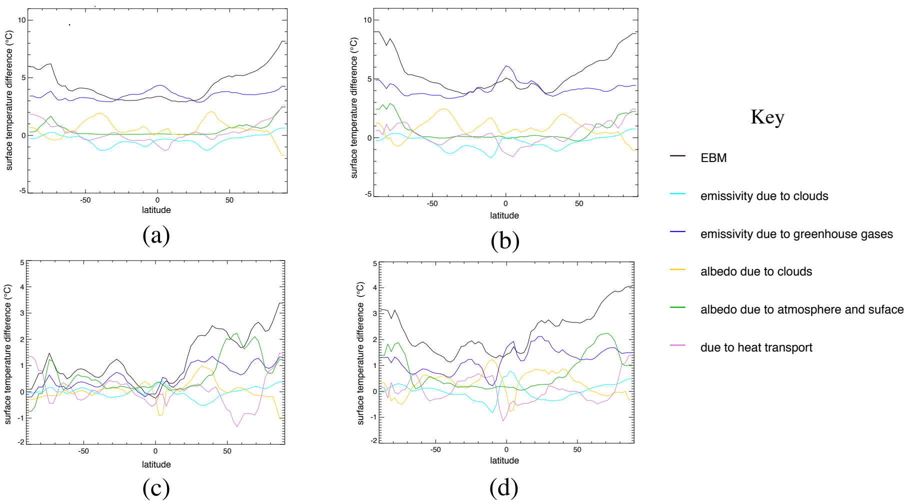

Fig. 13. Contributions from different factors to the annual mean temperature differences when CO_2 in doubled, determined through energy balance model analysis for **(a)** shrubs everywhere and **(b)** TRIFFID turned on and when land surface coverage changes from shrubs everywhere to the vegetation distribution predicted by TRIFFID determined through energy balance model analysis at **(c)** 2 × and **(d)** 4 × PI CO_2.

CPD
9, 4705–4744, 2013

Investigating vegetation-climate feedbacks during the early Eocene

C. A. Loptson et al.